



Idealized Simulations of Supercell Demise Based on VORTEX2 Observations

Casey E. Letkewicz and Matthew D. Parker

United States Air Force Academy and North Carolina State University

Introduction

The governing dynamics of supercells has been a long-standing area of active research, often with a focus on the developing and mature stages (e.g., Rotunno and Klemp 1982; Davies-Jones 1984; Weisman and Rotunno 2000). Supercell research has recently expanded to explore the processes behind weakening and dissipating supercells (Bluestein 2008; Ziegler et al. 2010), which may better inform our current understanding of supercell maintenance. Supercell decay has often been attributed to movement into cooler, stable air due to corresponding increases in CIN, making it more difficult to lift parcels to their LFCs (e.g., Bluestein 2008). However, the specific processes leading to weaker lifting are less certain.

On 9 June 2009, VORTEX2 sampled a supercell in south-central Kansas that produced strong low-level rotation and generated at least one reported tornado. However, an hour after the VORTEX2 armada deployed its various assets, the storm updraft was observed to shrink and completely dissipate. The goal of this study is to better understand the mechanisms and the circumstances that inhibit lifting of parcels to their LFCs, leading to storm demise.

Inflow Environment

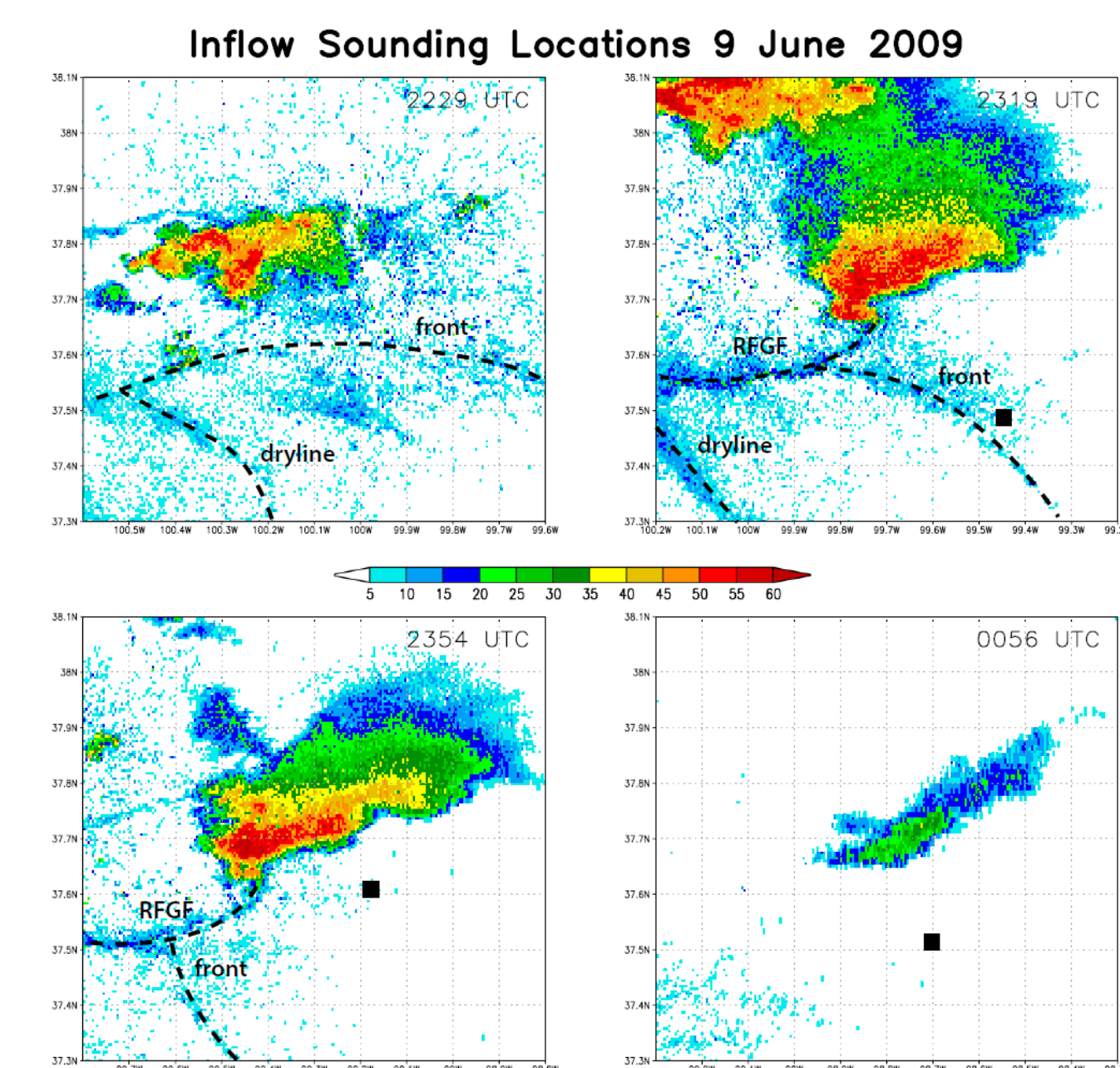


Fig. 1: Base reflectivity from the Dodge City WSR-88D depicting the evolution of the storm over time in relation to the launches of the near-inflow soundings (denoted by black squares in 3 of the panels, starting at 2319 UTC). The dashed lines represent various boundaries of interest, as detected by the radar finelanes, with the supercell's rear flank gust front ("RFGF"), the combined outflow boundary-synoptic front ("front"), and dryline labeled appropriately.

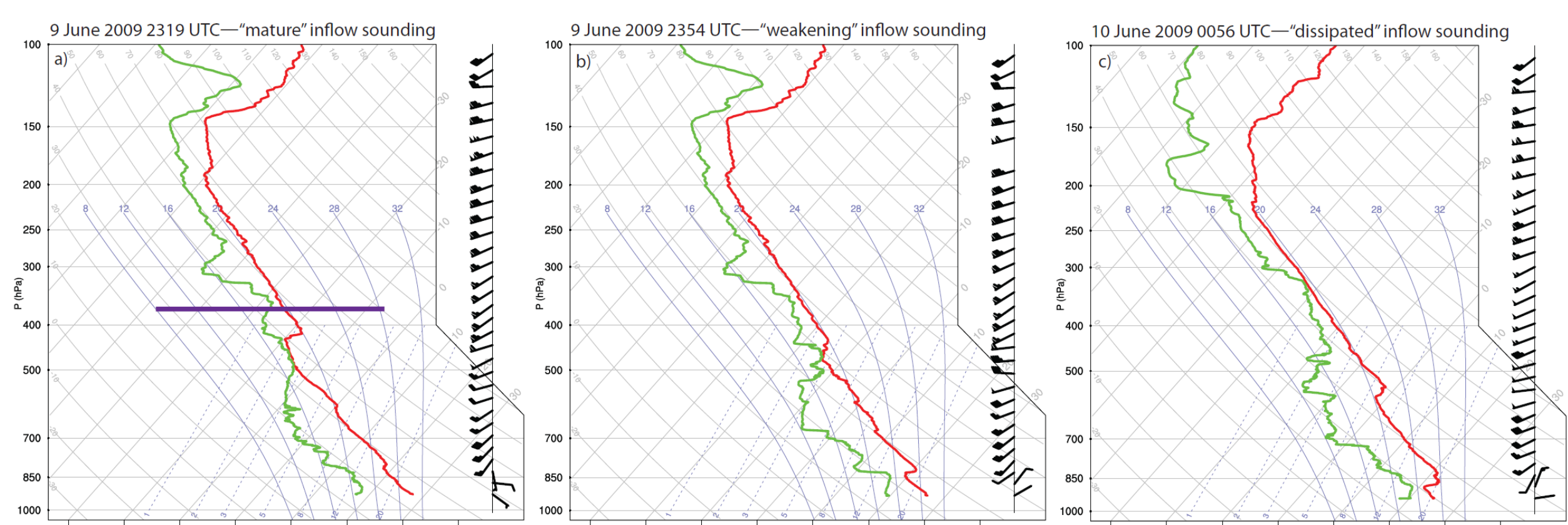


Fig. 2: Skew-T log-p diagrams of the soundings sampling the near-inflow environment 9-10 June 2009. The time of the launch and the storm's degree of maturity are indicated on each panel. The purple horizontal line in a) denotes the starting level where the sounding was modified using data from the 2354 UTC sounding in order to have data up through the tropopause.

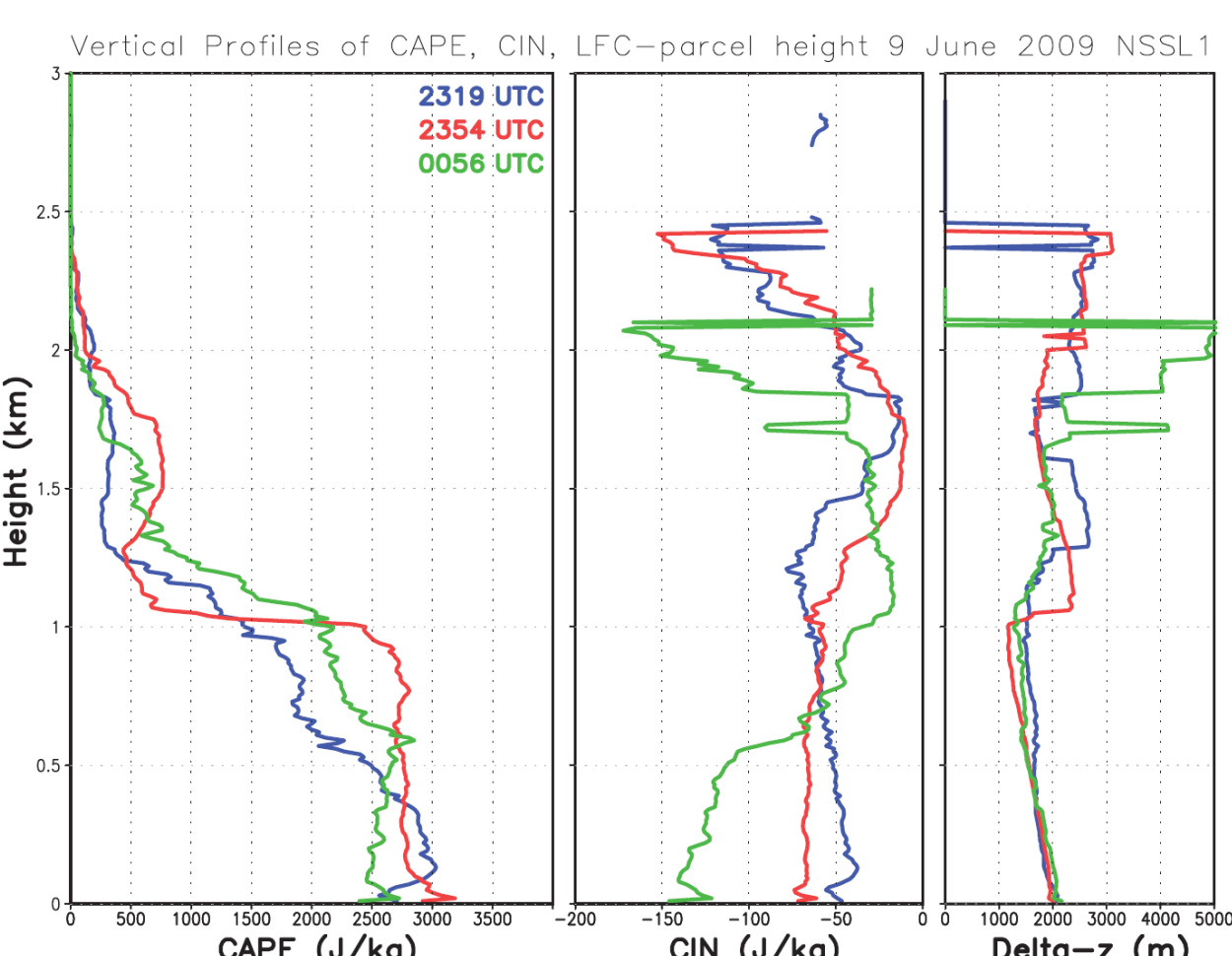


Fig. 3: Vertical profiles of CAPE, CIN, and delta-z (m; defined as vertical distance between parcel height & level of free convection) over time from the near-inflow soundings on 9 June 2009.

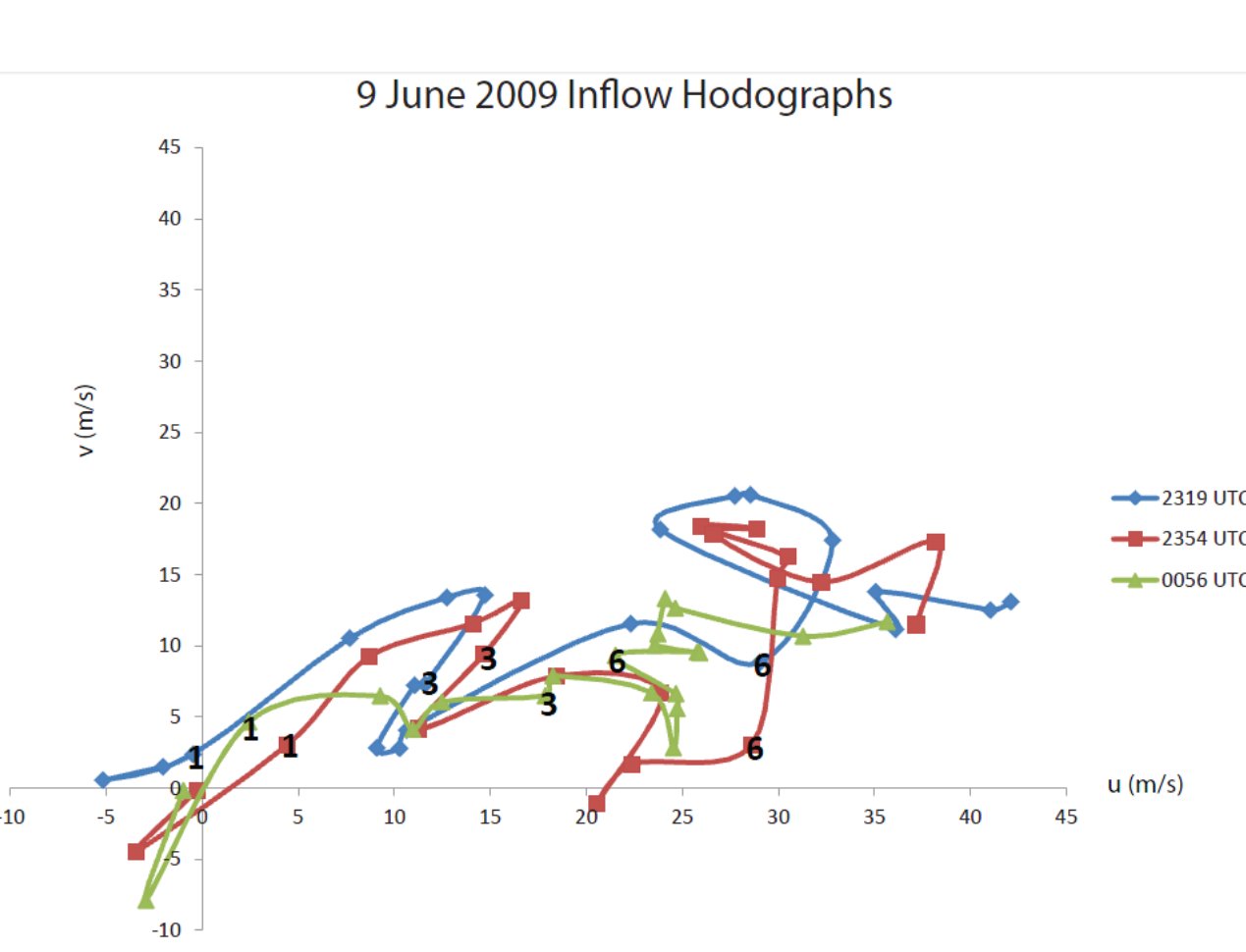


Fig. 4: Hodographs from the 9 June 2009 near-inflow soundings, with markers placed every 0.5 km, up to 10 km. Select levels (in km) are labeled for reference.

Modeling Technique

In order to examine the impact of the varying inflow environment on 9 June 2009 while still maintaining a degree of control over the experiments, a new modeling technique was developed called base-state substitution (BSS). After a certain amount of model run time, BSS replaces the originally homogeneous background environment with a new horizontally homogeneous environment while maintaining perturbations that developed during the preceding simulation (Fig. 5). This allows the user to independently modify the kinematic or thermodynamic environments, or replace the entire sounding without altering the structure of the perturbation fields. The environmental modifications can be incorporated gradually (gradual BSS) or instantaneously (instant BSS). For the simulations of the 9 June 2009 supercell, the supercell was allowed to mature for 3 hours before gradual environmental modifications were made, with the model restarted every 5 minutes and the environment changing a proportional amount.

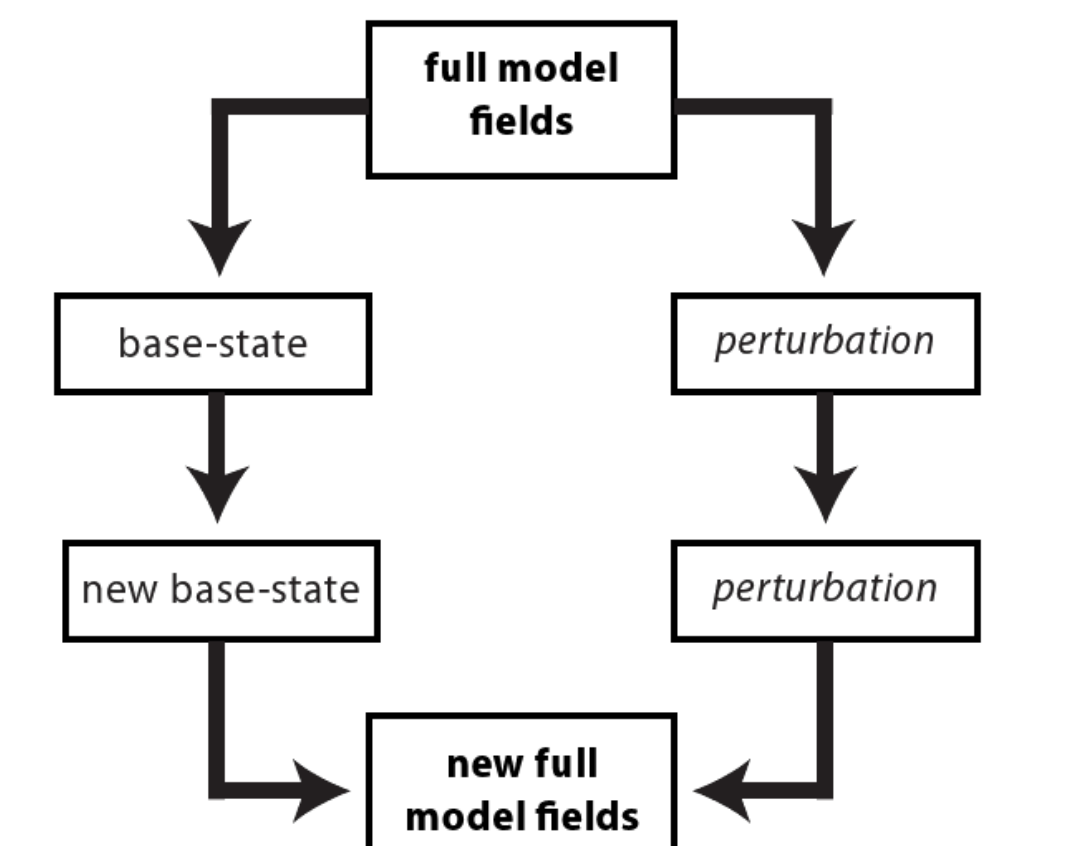


Fig. 5: Schematic of the procedure followed for base-state substitution.

Model Results

Combination Experiments (kinematic and thermodynamic changes)

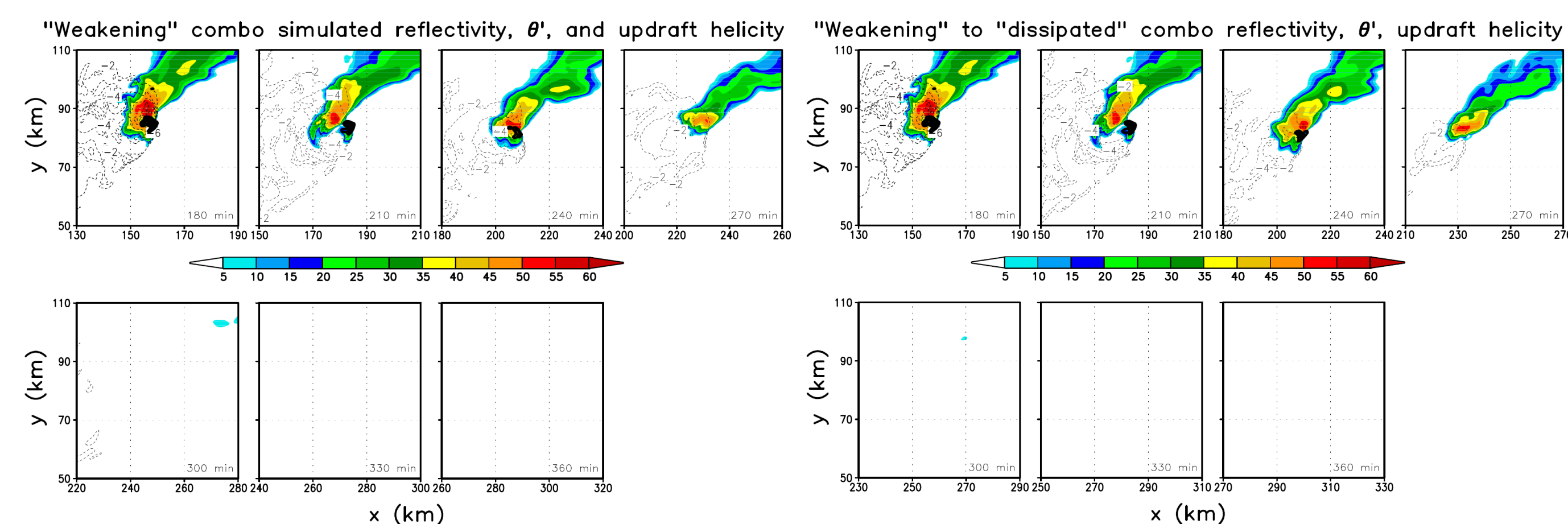


Fig. 6: Horizontal plan-view evolution of the second half of the "weakening" and "dissipated" combination simulations. Simulated radar reflectivity is shaded, θ is in the dashed contours every 2 K, and updraft helicity (calculated in the manner of Kain et al. 2008) is in the thick contours every 500 m^2/s^2 .

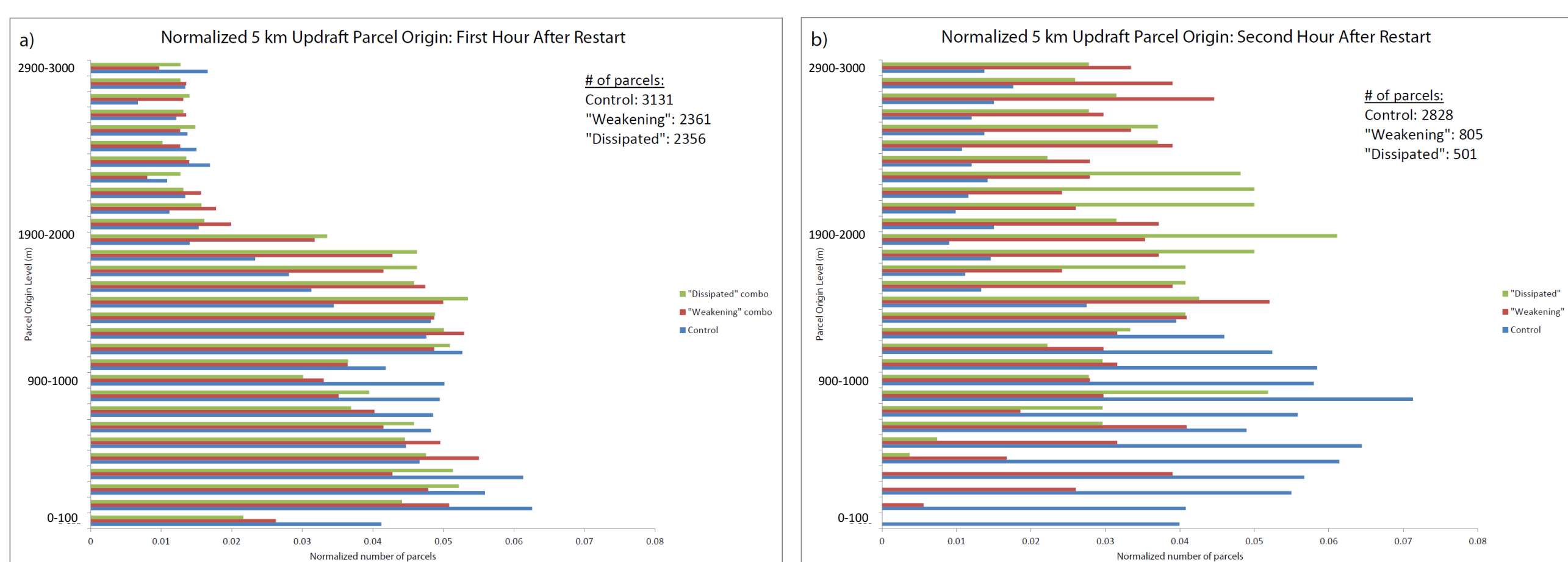


Fig. 7: Histograms of the normalized number of updraft ($w \geq 10$ m/s) parcels at 5 km binned by parcel origin level for the combination restart simulations during the a) first and b) second hour after the initial restart. The number of updraft parcels for each simulation is also listed on each panel.

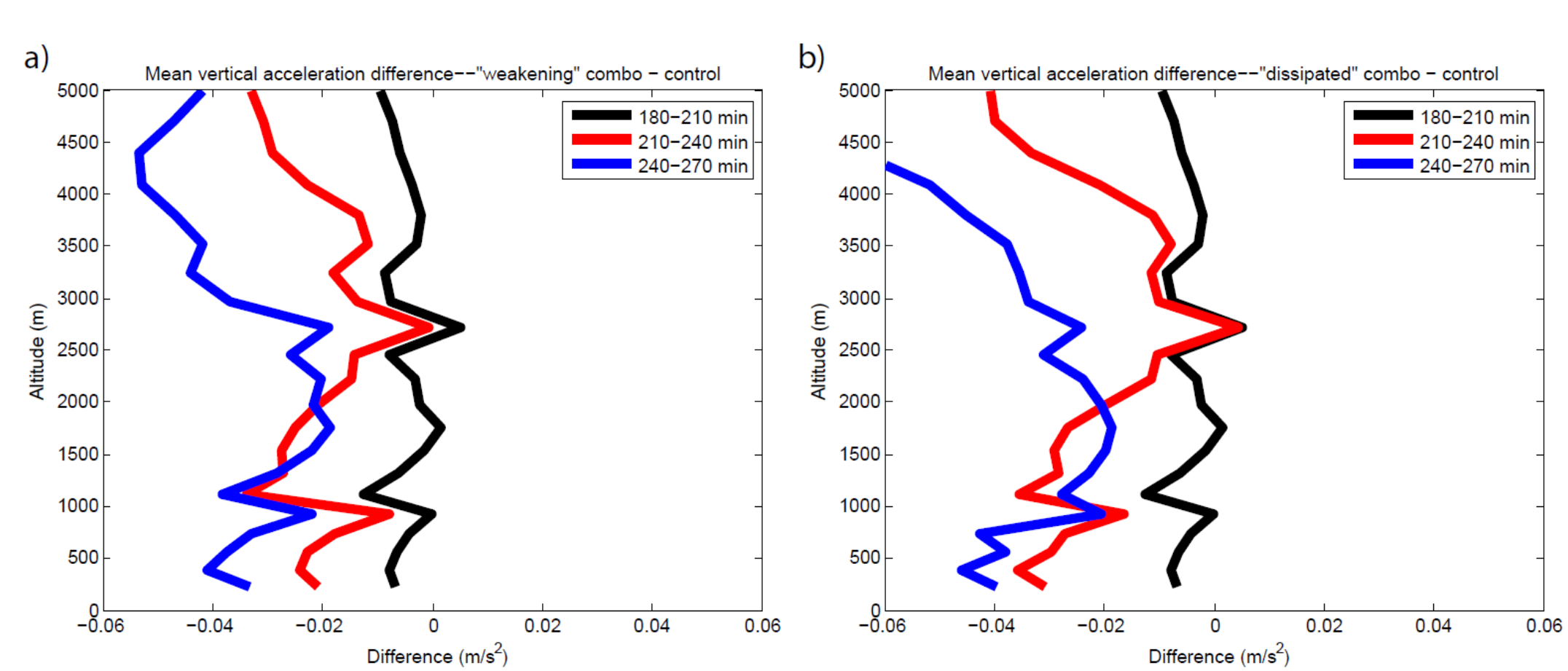


Fig. 8: The difference in total vertical acceleration (for grid points greater than or equal to the 99th percentile of vertical acceleration, m/s^2) between the combination experiments and the control. The mean difference is calculated for three 30 min increments (as labeled on the figure) after the environment began to be modified to demonstrate bulk changes.

Thermodynamic Experiments

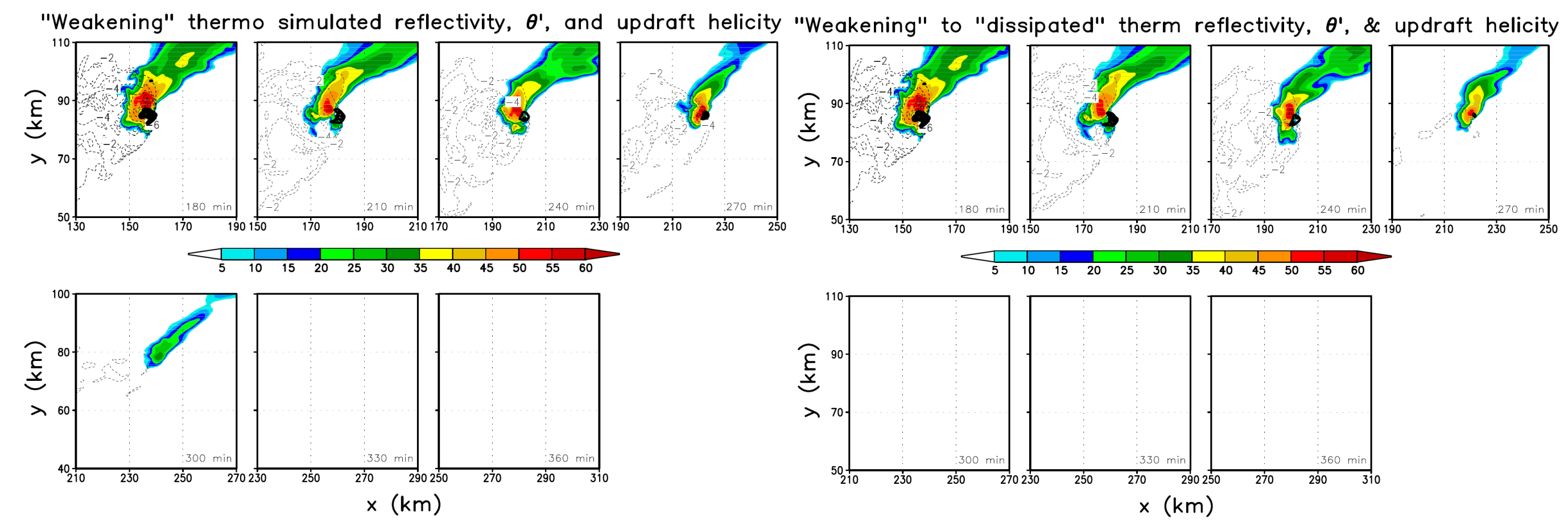


Fig. 9: As in Fig. 6, but for the "weakening" and "dissipated" thermodynamic simulations.

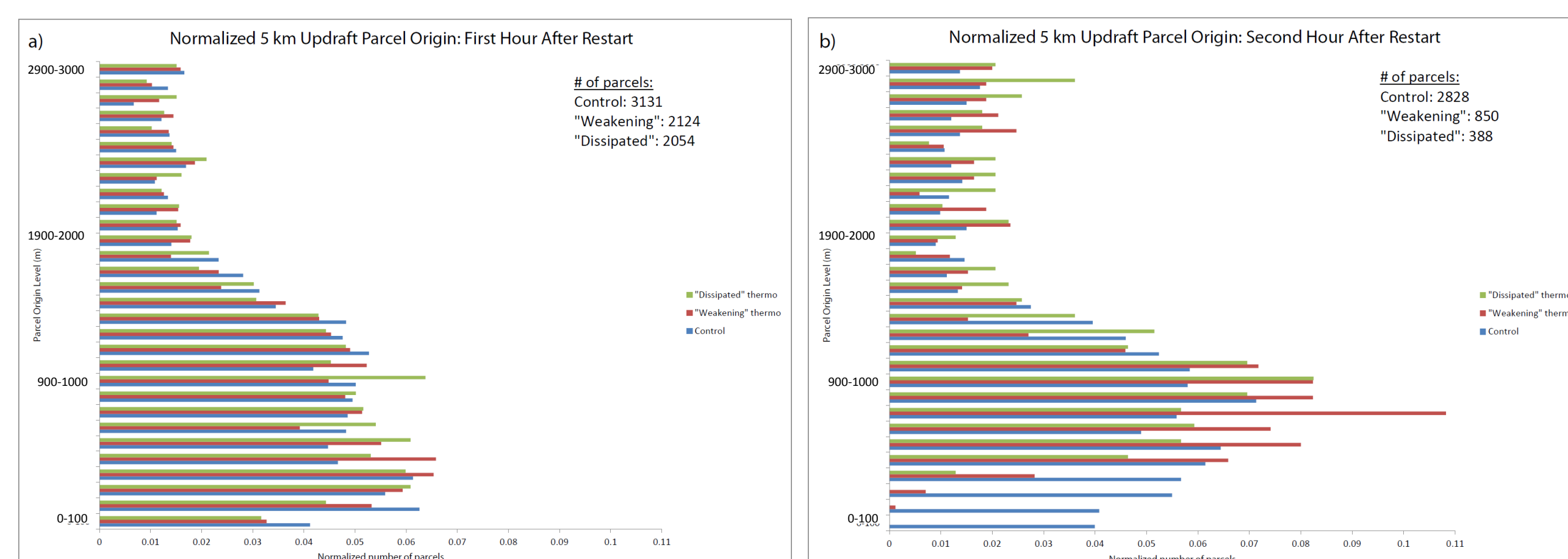


Fig. 10: As in Fig. 7, but for the thermodynamic restart simulations.

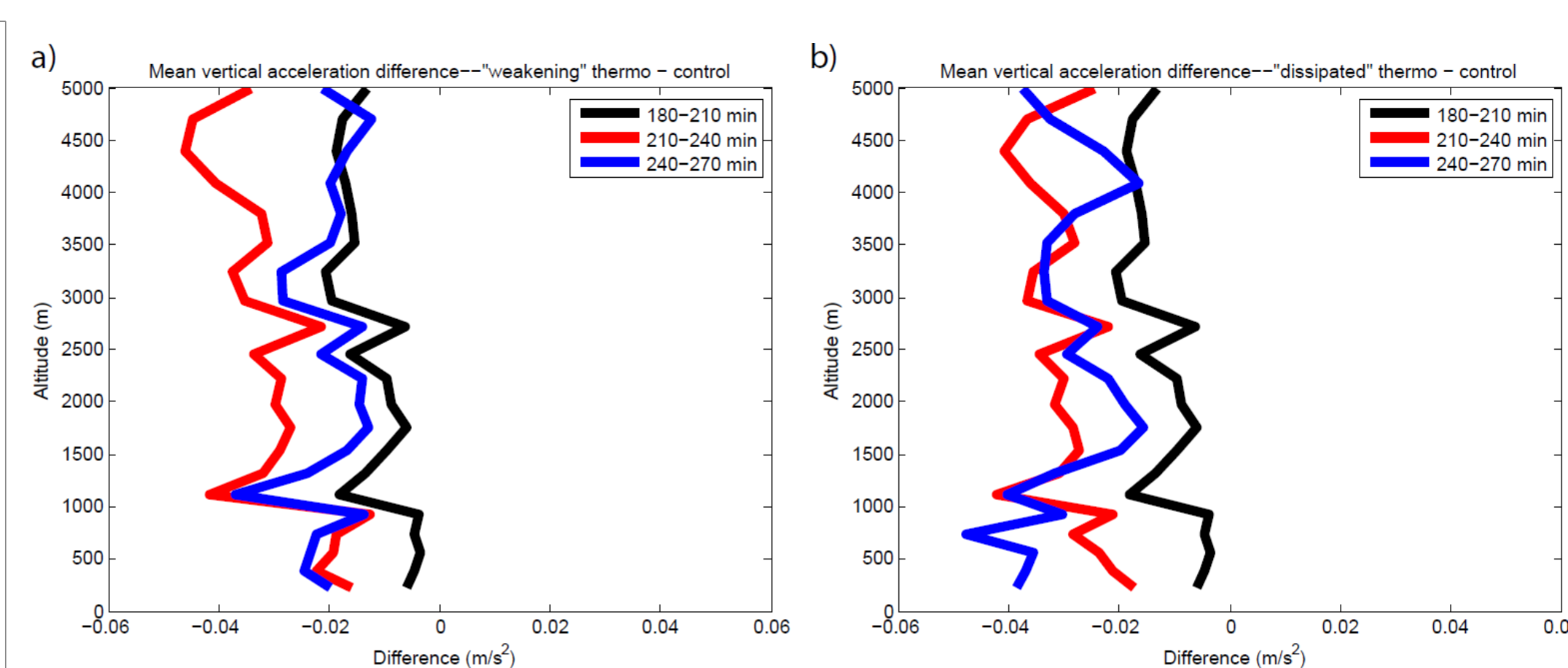


Fig. 11: As in Fig. 8, but for the thermodynamic restart simulations.

Wind Profile Experiments

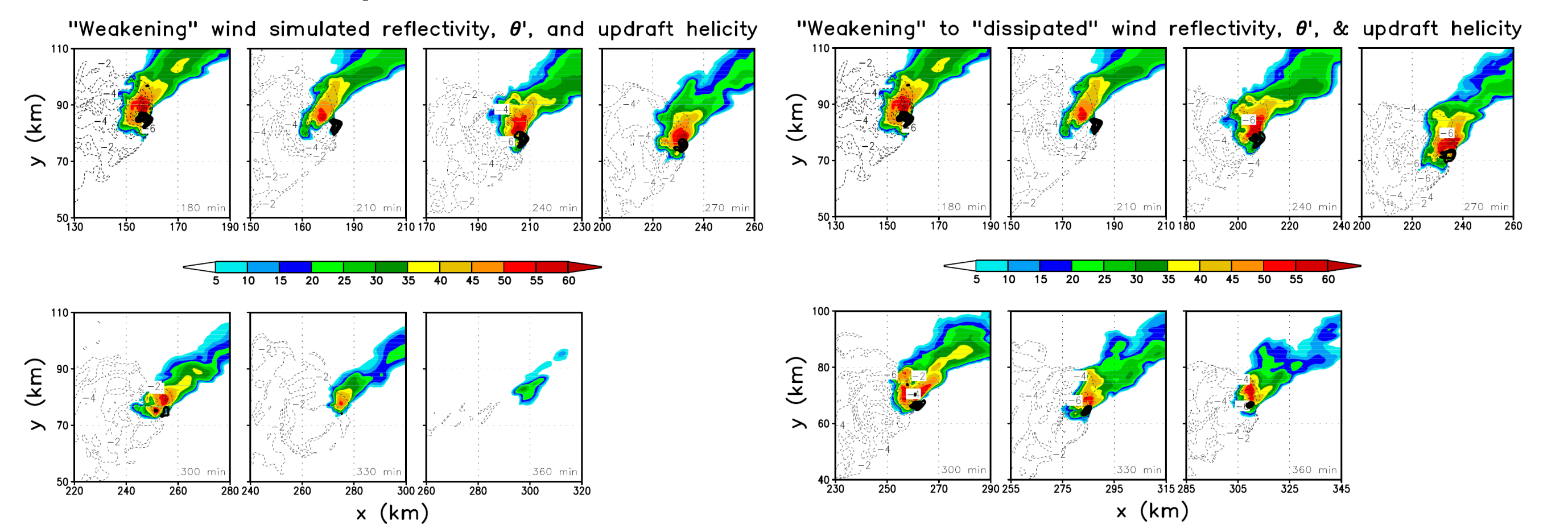


Fig. 12: As in Fig. 6, but for the "weakening" and "dissipated" wind profile simulations.

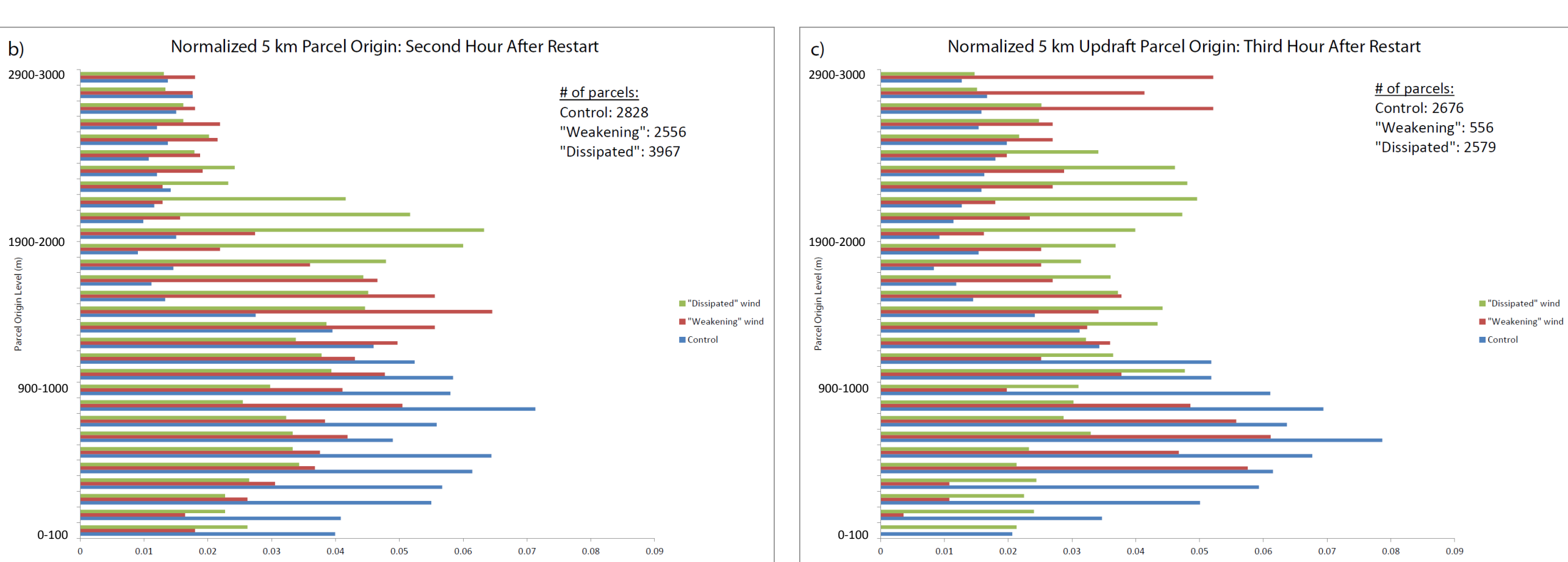


Fig. 13: As in Fig. 7, but for the wind profile restart simulations. Note that the panels shown are for the second and third hours after the initial model restart.

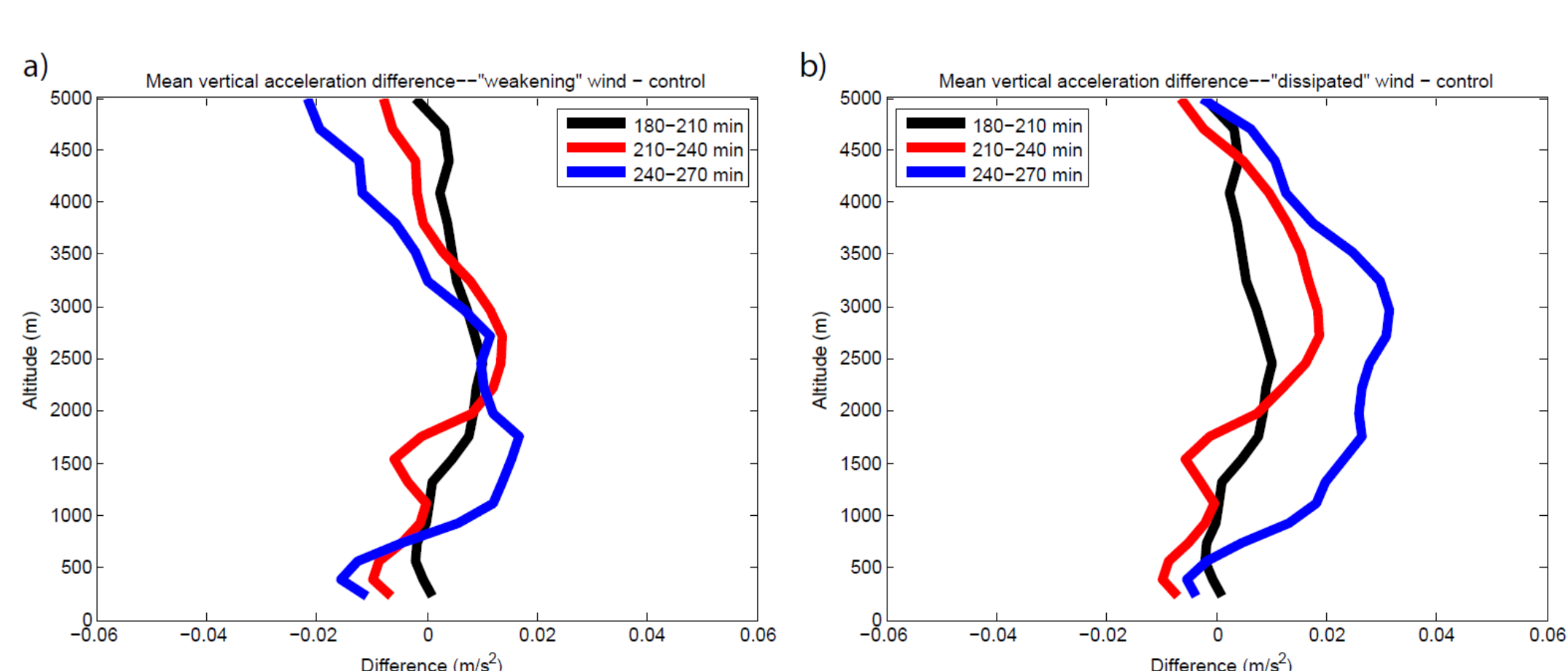


Fig. 14: As in Fig. 8, but for the wind profile restart simulations.

Conclusions and Future Work

The experiments demonstrated that the demise of the 9 June 2009 supercell was primarily due to the thermodynamic modifications to the environment, though wind profile changes also impacted the simulated storm. Increasingly stable low-levels made it more difficult for low-level parcels to be lifted to their LFCs, and also weakened the cold pool, resulting in weaker low-level lifting. These changes led to an upward shift in the source region for updraft parcels, as well as a reduction in the total number of updraft parcels. Changes to the wind profile also contributed to shifting the updraft parcel source region, which lead to the storm ingesting drier, elevated parcels. Consequently, updraft buoyancy was reduced and the storm eventually dissipated.

There are a number of avenues that should be explored to further understand the interplay of thermodynamic and kinematic changes in the environment and subsequent impacts on storm dynamics and maintenance. One such possibility includes testing a wide variety of thermodynamic and kinematic environment combinations, such as simulating a supercell in an increasingly cool low-level environment while increasing shear and helicity. Additionally, given the role of drier parcels in reducing updraft buoyancy, future simulations should utilize a smaller resolution in order to more faithfully represent entrainment. Finally, there is still much to be understood concerning environmental heterogeneity and subsequent storm morphology, and we encourage future studies to utilize the powerful BSS modeling technique.

Acknowledgements

The authors would like to thank Drs. Anantha Aiyer, Gary Lackmann, Sandra Yuter, and Conrad Ziegler for their helpful suggestions and assistance with this work. The Convective Storms Group at NCSU is also acknowledged for their support and useful feedback. This work is supported by NSF Grant AGS-0758509 and AGS-1156123.